Polarization and Wavelength Performance Improvement in Large-Scale Silicon Photonics Switches

Keijiro Suzuki, Ryotaro Konoike, Hiroyuki Matsuura, Ryosuke Matsumoto, *Member, IEEE*, Takashi Inoue, Shu Namiki, *Fellow, IEEE*, Hitoshi Kawashima, and Kazuhiro Ikeda, *Member, IEEE*

(Invited Paper)

***Abstract*—We review our recent results in multi-port strictly non-blocking optical switches based on silicon photonics. Silicon photonics switches are one of the most important devices to realize future datacenters capable of processing a large amount of data with high efficiency. This is because silicon photonics enables fast (ns - μs) switching, dense integration with high uniformity, low power consumption, and mass production leading to low cost. Thus far, we demonstrated switching, all-paths transmission, and fully-loaded operation of up to 32 input ports $\times$ 32 output ports silicon photonics switches. The remaining challenges for practical applications are polarization insensitivity and broadband operation. Regarding the polarization-insensitivity, we presented the non-duplicated polarization-diversity 32 $\times$ 32 switch with SiN over path waveguides and demonstrated polarization-insensitive operation in limited paths. Regarding the broadband operation, we achieved $\sim$90 nm bandwidth for $-$30 dB crosstalk with polarization-insensitivity in the 8 $\times$ 8 switch. We review these, and then discuss how to achieve a large port count ($>$32 $\times$ 32), polarization-insensitivity, and broadband operation simultaneously. Moreover, to broaden the range of applications, integration with wavelength filters and expanding operating wavelengths are important. We demonstrated hybrid integration with the silica platform that is suitable for wavelength filters and the 8 $\times$ 8 switch operating in the O-band.**

***Index Terms*—Optical switches, photonic integrated circuits, strictly-non-blocking switches.**

I. Introduction

THE data flow within data centers has increased with the recent spread of on-demand movies, cloud-based services, and teleworking. Furthermore, the availability of new devices such as AI accelerators will require even greater transmission capacity in the future. To meet this throughput demand, one of the key components is the network switch, because network switches and optical fiber links connect many servers. In this situation, the application-specific integrated circuit in the network switch has expanded its bandwidth at a rate of doubling in every two years and reaching 25.6 Tb/s [1]. This bandwidth expansion occurs along with an increase in electric power con sumption, which is a bottleneck for further bandwidth expansion. Hence, to continue scaling up the bandwidth with reasonable power consumption, technological breakthroughs are required. One technology that is expected to overcome these bottlenecks is optical switching. One of the reasons is that the power consumption of the optical switches is not proportional to the symbol rate of the transmitting signals but to the port counts. Some researchers have proposed network systems that exploit optical switches [2], [3], [4].

A silicon photonics platform is one of the most suitable options for optical switches because it offers many advantages: fast (micro-to nanoseconds) switching, large-scale integration with high uniformity, and mass production. Thus far, the maximum port counts we reported were 32 input ports $\times$ 32 output ports, which exhibited an average fiber-to-fiber insertion loss of 10.8 dB [5]. The basic components are 2 $\times$ 2 Mach-Zehnder (MZ) switches with thermo-optic phase shifters and adiabatic intersections [6]. These basic components are aligned to form a path-independent insertion loss (PILOSS) topology [7]. The 32 $\times$ 32 switch was tested under fully loaded conditions, and we demonstrated 0.29 pJ/bit wall-plug efficiency and 81.9 Tb/s throughputs [8]. These performances exceed those of electric switches, as shown in Fig. 1. However, the 32 $\times$ 32 switch can operate only for transverse-electric (TE) polarization and its bandwidth is narrow (3.5 nm for $-$20 dB crosstalk). Therefore, polarization insensitivity and broadband operation are future challenges. Regarding polarization insensitivity, our approach involves a polarization-diversity scheme [9] in which two identical switch matrices are used for the two orthogonal polarizations. As a preliminary demonstration, we prepared two sets of optical switches and their control electronics, and demonstrated polarization-insensitive operation by combining them [10]. Recently, we demonstrated a single-chip integration version of a polarization-diversity 8 $\times$ 8 switch [11]. Moreover, we propose a polarization-insensitive 32 $\times$ 32 switch with a single-switch matrix [12]. For broadband operation, a double-MZ element

Manuscript received 30 May 2022; revised 25 August 2022; accepted 2 September 2022. Date of publication 7 September 2022; date of current version 2 February 2023. *(Corresponding author: Keijiro Suzuki.)*

The authors are with the Advanced Industrial Science and Technology, Tsukuba 305-8569, Japan (e-mail: k.suzuki@aist.go.jp; r.konoike@aist.go.jp; hiroyuki.matsuura@aist.go.jp; matsumoto.ryosuke@aist.go.jp; inoue.takashi@aist.go.jp; shu.namiki@aist.go.jp; kawashima-h@aist.go.jp; kaz.ikeda@aist.go.jp).

Color versions of one or more figures in this article are available at https://doi.org/10.1109/JLT.2022.3204810.

Digital Object Identifier 10.1109/JLT.2022.3204810

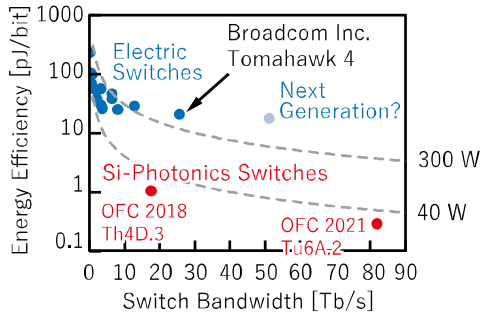

Fig. 1. Comparison of energy efficiency and switch bandwidth among electrical and optical switches.

switch, in which the two MZ switches are cascaded, is suitable for the PILOSS topology [13]. We demonstrated a bandwidth of $\sim$ 90 nm for a crosstalk bandwidth of -30 dB [11].

In this study, we review our recent progress in the polarization-insensitive and broadband operation of silicon photonic switches and discuss how to achieve this in a large port-count switch, such as 32 $\times$ 32 ports. In the following sections, we focus on polarization diversity 32 $\times$ 32 switch with a non-duplicated diversity scheme and polarization-diversity double-MZ 8 $\times$ 8 switch. Furthermore, the integration of other functions, such as wavelength filters and the extension of the operating wavelength range, is important for increasing the applicability of optical switches. We demonstrated a hybrid integration with a silica planar lightwave circuit (PLC) that can offer commercially acceptable performance filters and an O-band operation that is prevalent in data center networks. We also review these two technologies, which are extensions of the review in [14].

II. Nonduplicate Polarization-Insensitive 32 $\times$ 32 Switch

We believe that the polarization-diversity scheme is one of the most practical options for achieving polarization-insensitive operation because it does not require a high fabrication accuracy that is essential for making silicon photonic components polarization insensitive. In the polarization-diversity scheme, two identical switch matrices are used to handle two orthogonal polarizations. This may become a problem for large port-count switches because the electrodes for the element switches and the footprint of the switch matrix are doubled. To avoid these drawbacks, we propose a non-duplicated polarization-diversity structure that bidirectionally utilizes the PILOSS topology [15]. Moreover, to eliminate many intersections for bidirectional routing on the switch chip, we integrated the SiN overpass waveguides above the Si waveguide layer.

Fig. 2(a) shows the fabricated non-duplicated polarization diversity 32 $\times$ 32 switch chip [12]. A total of 74 (input:32, output:32, test device:8, Si waveguide for fiber-array alignment) edge couplers were fabricated on the left side of the chip and connected to a polarization splitter/rotator (PSR), which is based on an asymmetric structure and directional coupling [16]. In PSR, the TE and TM modes are separated, and then the original TM mode is rotated to the TE mode (all the propagating light through

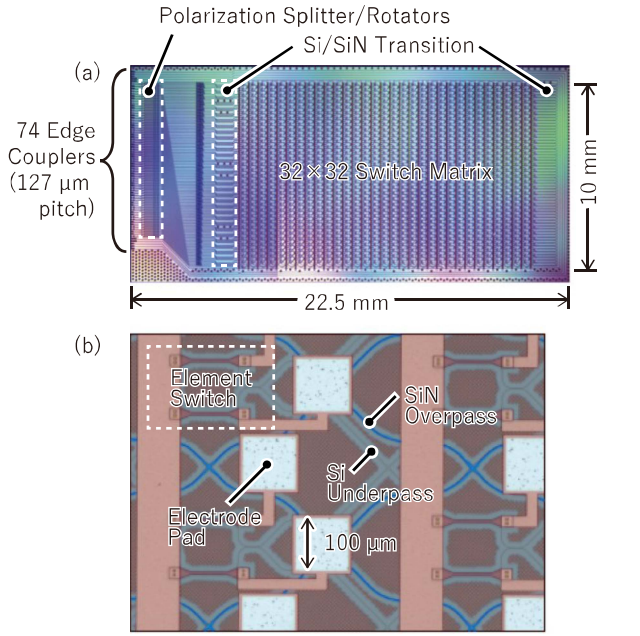

Fig. 2. (a) Microscopy image of fabricated non-duplicated polarization-diversity 32 $\times$ 32 switch chip. (b) Magnified image of element Mach-Zehnder switches, upper SiN waveguides, and electrodes.

the chip is TE mode). The original TE mode (X component) was transferred to the SiN overpass waveguide (Fig. 2(b)) using a SiN/Si transfer coupler. The X component then propagates to the right side of the chip and is transferred to the Si waveguide layer with another SiN/Si transfer coupler. Subsequently, the X component propagates through the switch matrix and reaches the output PSR. In contrast, the original TM mode (Y component) propagates through the switch matrix and is then transferred to the SiN overpass layer with a SiN/Si coupler on the right side. Subsequently, the Y component propagates the SiN overpass waveguide, transfers the Si waveguide with the output SiN/Si coupler, and reaches the output PSR. In the output PSR, the X component is rotated to the TM mode and the Y component propagates through without any changes.

Fig. 3(a) shows the polarization-dependent losses (PDLs) of sampled 32 paths, which are chosen so that the input and output ports are not adjacent to each other to prevent interference between the scattered input light and output light. The average PDL was 3.5 dB and 75% of the measured PDLs were less than 3 dB. We suspect that the interference between the light propagating through the established paths, the leakages from the path of the oppositely polarized component in the switch matrix, and the insufficient polarization splitting and rotation in the PSR degrade the PDL. Therefore, optimization of the device and fabrication process can improve the PDL. Fig. 3(b) shows the measured differential group delay (DGD) of path 23 – 23. The measured DGD is 1.7 ps. In this switch topology, the propagation lengths of all the paths are identical. Therefore, a 1.7 ps DGD can be expected for all paths.

Here, we discuss the merits and demerits of the nonduplicated diversity scheme. The largest merit of this switch topology is that polarization diversity is possible without doubling the

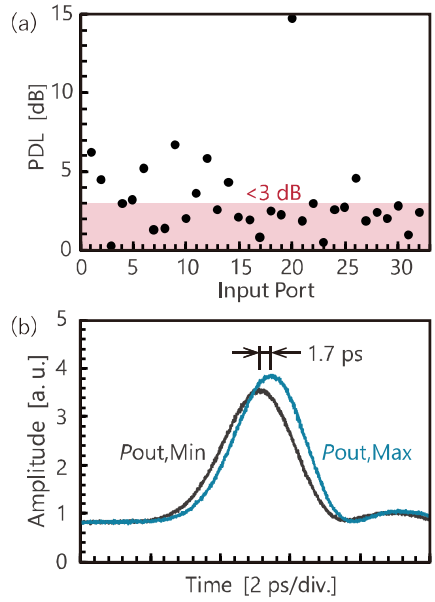

Fig. 3. (a) Measured polarization dependent loss of fabricated 32 × 32 switch. Measured paths: 1 (input) - 1' (output), 2 – 2', 3 – 3', …, 32 – 32'. (b) Observed optical pulses propagating through 23 – 23' in cases of maximum and minimum output powers. The output powers were adjusted by controlling the polarization of input pulses.

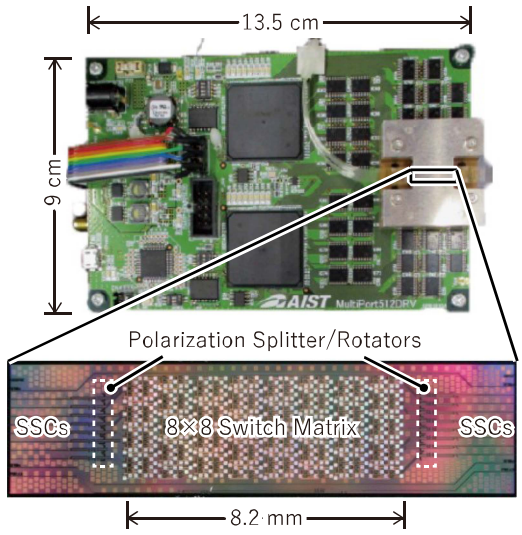

Fig. 4. Polarization-diversity double Mach-Zehnder 8 × 8 switch assembled onto printed circuit board with control electronics. The magnified switch chip is shown at the bottom of the figure.

number of element switches. This is a desirable feature for element switch counts that exceed 1000, such as 32 × 32 port switches. Although the present operational demonstration was limited due to imperfect polarization extinction ratios in the polarization splitter rotators, by optimizing them we think we could demonstrate characteristics similar to those reported in [5] for each polarization. One demerit is that it is difficult to achieve wideband operation above 15 nm. Broadband operation requires a double MZ element switch, in which two MZ switches are connected successively as described in the next section, however the configuration of this topology precludes its use. However, the nonduplicated topology could be used for narrow bandwidth schemes such as LAN-WDM (1306 – 1318 nm).

III. Polarization and Wavelength Insensitive 8 × 8 Switch

Fig. 4 shows a polarization-insensitive broadband 8 × 8 switch [11]. To achieve polarization insensitivity, we used a polarization diversity scheme. Two identical 8 × 8 switch matrices are nested (we call nested type), simplifying the connection of the routing waveguide. To achieve broadband operation, we used a double-MZ element switch [13], which comprises two cascaded MZ switches and an intersection. Therefore, the leakage from the MZ switch underwent suppression twice, resulting in low crosstalk and broad bandwidth.

The switch chip, which was fabricated by AIST's pilot line, was flip-chip bonded to a ceramic interposer and then inserted into a socket on a printed circuit board (PCB). The PCB has two FPGAs that generate 1 MHz electric pulses. The width of the electric pulses was controlled to adjust the electric power applied to the heater phase shifters on the switch chip. The size of the assembled 8 × 8 switch was 13.5 cm × 9 cm, which is comparable to that of a smartphone.

We evaluated fiber-to-fiber insertion loss, crosstalk, PDL, and DGD. The average and minimum fiber-to-fiber insertion loss was 11.9 dB and 11.0 dB, respectively. A major part of the insertion loss was the fiber-to-chip coupling (∼5 dB). Hence, the optimization of the edge coupler may improve the insertion loss. Fig. 5(a) shows the crosstalk spectrum of one of the most severe paths. Crosstalk of less than −30 dB was obtained in the wavelength range of 90 nm. Fig. 5(b) and (c) show the measured worst PDL and DGD of path 7 – 6', respectively. Theoretically, the PDL for any path should be the same. However, due to variations in the polarization extinction ratio of the PSRs and their combination, a worst case exists. The PDL and DGD were less than 0.4 dB and 1.8 ps in a wavelength range from 1.52 to 1.6 μm, respectively.

Here, we discuss the merits and demerits of the duplicated diversity scheme. Although the merits and demerits of the nested type are inversely related to those of the nonduplicated type, the merit of the nested type is that a wider bandwidth can be achieved by using double MZ element switches. As shown in Fig. 5, an 8 × 8 switch can provide less than −30 dB of crosstalk in a wide bandwidth of about 90 nm. Therefore, a duplicated type is needed to realize a switch that can operate in the entire O-, C-, and L-band range, for example. The disadvantage is that the number of element switches increases. Since the number of electrodes also increases, technology capable of handling them is required. This is discussed in Section V.

IV. Expanding Application Fields of Silicon Photonics Switches

In this section, we describe some technologies to expand applications of silicon photonics switches. Especially, we focus on two technologies: hybrid integration with silica PLCs

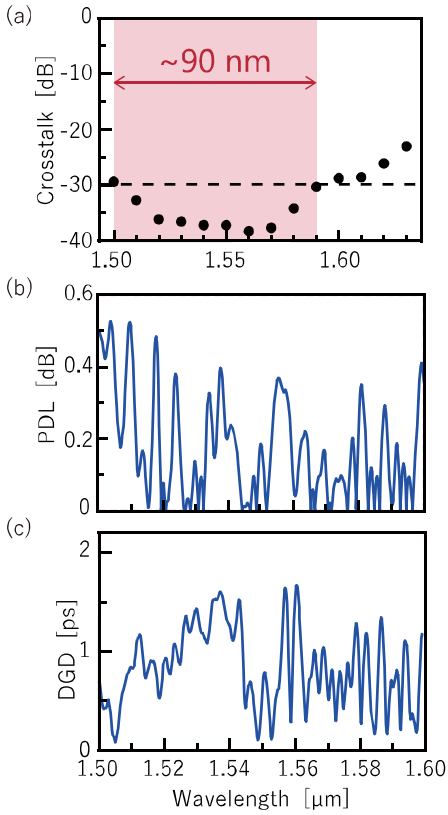

Fig. 5. (a) Measured one of the worst crosstalk spectra of the fabricated 8 × 8 switch. (b) Wavelength dependence of polarization-dependent loss. (c) Differential group delay. The measured path of PDL and DGD was input port 7 to output port 6', in which are the worst cases.

and O-band operation. The silica PLC platform can provide a high-performance wavelength filter that can be accepted at the commercial application level and is difficult for the silicon photonics platform. The O-band operation has recently become important because the demand for optical switches in the data center is increasing. The reviews of these two technologies are described below.

A. Hybrid Integration With Silica PLC

In silicon photonics, the high refractive index contrast between the core and cladding enables large-scale photonic integration with a compact size, low power consumption, and low-cost manufacturing. However, its strong optical confinement to the core has some disadvantages, such as modal field incompatibility with optical fibers and large phase errors in interferometers, gratings, and resonators. Conversely, the silica PLC platform can provide a fiber-compatible modal field and a small phase error, which are commercially acceptable. Therefore, the hybrid integration of silicon photonics and silica PLC can compensate for each other's limitations and benefit from each other's advantages. In this concept, we demonstrated a wavelength (DE)MUX-and-switch device consisting of a polarization-diversity double-MZ 8 × 8 silicon photonic switch and a SiO_2-ZrO_2-based (5.5% Δ) 100-GHz 8-ch arrayed waveguide grating (AWG) [17].

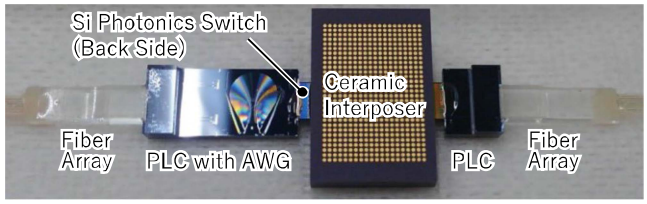

Fig. 6. Hybrid device of 5.5%-Δ planar-lightwave-circuit (PLC) chip and silicon-photonics chip. The PLC chip has arrayed waveguide grating (AWG). The silicon chip has polarization-diversity double Mach-Zehnder 8 × 8 switch. The hybrid device is capable of wavelength (DE)MUX-and-switch, and switch-and-MUX functions.

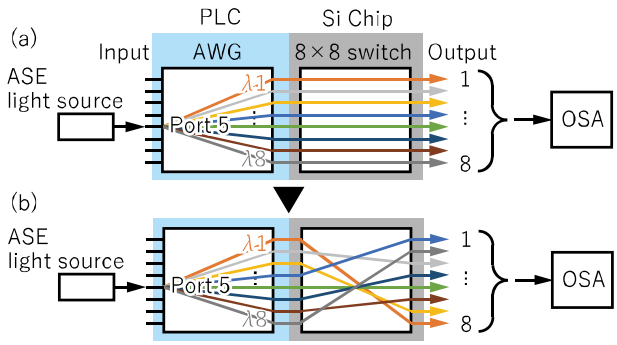

Fig. 7. Schematics of wavelength DEMUX-and-switch operation. (a) Switch state 1. 1 (input) –1' (output), 2 – 2', 3 – 3', 4 – 4', 5 – 5', 6 – 6', 7 – 7', and 8 – 8'. (b) Switch state 2. 1 – 8', 2 – 3', 3 – 7', 4 – 1', 5 – 5', 6 – 4', 7 – 6', 8 – 2'.

Fig. 6 shows assembled device chip with a ceramic interposer. The PLC with AWG was butt-jointed to silicon photonics switch chip. Here, the modal field diameter for the butt-joint was set to 3 μm, which is acceptable for the 5.5%-Δ silica PLC [18] and silicon photonics. The ceramic interposer was inserted into a land-grid-array socket on a PCB.

Fig. 7 shows the wavelength DEMUX and switch operation. The unpolarized broadband light from the ASE light source is divided into eight wavelength channels. Each channel output was connected to the input port of an 8 × 8 switch. The switch state was set to state 1 (Fig. 7(a)) or state 2 (Fig. 7(b)). The wavelength spectrum of the output light was observed using an optical spectrum analyzer. Fig. 8 shows the fiber-to-fiber transmission of the hybrid device in switch states 1 and 2. We did not observe any spectral degradation for either switch state. These results indicate that this hybrid platform has the potential for compactness, low power consumption, fast switching, and good device performance.

B. O-Band Operation

In data center network applications, the O-band (1260 – 1360 nm) is commonly used (e.g., 400G CWDM8 [19], 400GBASE-LR/FR8 [20]). This is because it does not require dispersion compensation techniques, such as digital coherent demodulation, resulting in a low cost. Therefore, when considering applications in data centers, it is important to design switches to operate in the O-band.

Fig. 9 shows the fabricated double-MZ 8 × 8 switch for the O band. For the O-band operation, the waveguide core dimensions

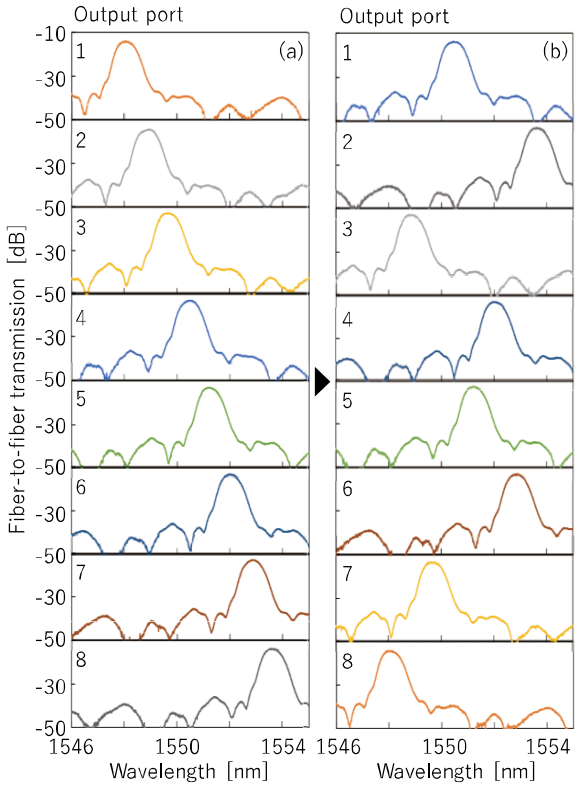

Fig. 8. Fiber-to-fiber transmission spectra of hybrid device at switch state 1 (a) and 2 (b), shown in Fig. 6.

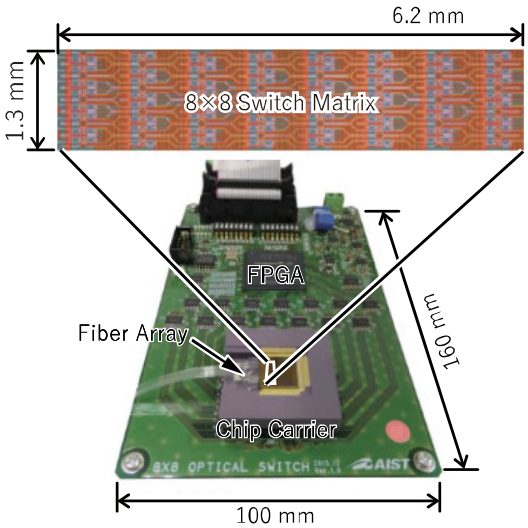

Fig. 9. Double Mach-Zehnder 8 × 8 switch operating in O-band. The magnified switch chip is shown in the top of figure.

were 320-nm-wide and 220-nm-thick. The propagation loss in TE-mode was 2.1 dB/cm. Using the waveguide, we composed the element MZ switches and intersections, which exhibited almost the same characteristics as at a wavelength of 1.55 μm.

The average fiber-to-fiber insertion loss were 16.6 dB. In this preliminary trial, we used an edge coupler designed for wavelength of 1.55 μm (5.6 dB/facet). Hence, if we used the edge coupler designed for the O-band (2.3 dB/facet), a fiber-to-fiber

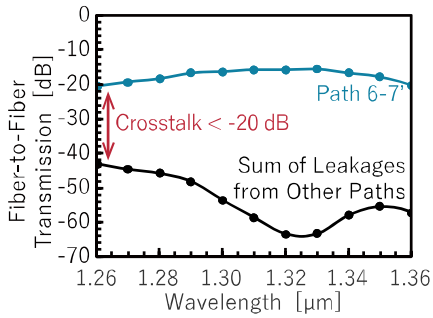

Fig. 10. Fiber-to-fiber transmission spectra of path 6 (input) – 7' (output) and sum of leakages from other paths. Path 6 – 7' is one of the worst crosstalk paths.

insertion loss of less than 10 dB could be feasible. Fig. 10 shows the spectra of the fiber-to-fiber insertion loss of path 6 – 7' and the sum of leakages from other paths. Path 6 – 7' is one of the most severe crosstalk paths. Less than −20 dB crosstalk was achieved in the entire O-band. Moreover, less than −30 dB crosstalk was obtained over a bandwidth of 70 nm.

V. Discussion

As discussed above, we achieved large-scale, polarization-independent, and broadband operations. Our next challenge is to achieve these characteristics simultaneously. One of the largest obstacles is the fan-out of electrodes on the switch chip. The fabricated 32 × 32 switch had 2112 electrodes. The number of electrodes was doubled by adopting a double-MZ element switch. Moreover, by composing the polarization-diversity scheme, the number of electrodes was further doubled. Therefore, we must achieve a fan-out of more than 8000 electrodes from the chip. This number is larger than that for the latest CPU packaging (e.g., LGA 3647). To realize a polarization-insensitive broadband 32 × 32 switch, a new packaging technology that can handle such a large number of electrodes is necessary. We think that one of the candidates for fan-out of many electrodes is the Si interposer [21]. The Si interposer is based on through-Si-via technology and can realize fine wiring which is difficult with conventional ceramic substrates. Otherwise, the integration of control circuits and silicon photonic switches into a single chip may be an alternative [22].

VI. Conclusion

We reviewed our recent results for strictly non-blocking silicon photonic switches. Thus far, we have demonstrated a 32 × 32 switch. Regarding polarization insensitivity and broadband operation, we demonstrated up to an 8 × 8 switch scale. To realize polarization insensitivity and broadband operation in a 32 × 32 switch, we pointed out that fan-out of more than 8000 electrodes is one of the largest obstacles. To overcome this, we need to develop new packaging technology that can deal with a large number of electrodes or one-chip integration with a control electric circuit. When considering data center applications, a silicon photonic switch operating in the O-band is important. We confirmed that the O-band operation can be achieved by optimizing the design parameters. As mentioned above, some

problems remain to be solved. However, we believe that silicon photonic switches can pave the way for future energy-efficient data-center networks.

REFERENCES

[1] For example, Broadcom web page, 2022. [Online]. Available: https://www.broadcom.com/products/ethernet-connectivity/switching/strataxgs/bcm56990-series

[2] K.-I. Sato, "Realization and application of large-scale fast optical circuit switch for data center networking," *J. Lightw. Technol.*, vol. 36, no. 7, pp. 1411–1419, Apr. 2018.

[3] K.-I. Kitayama et al., "Torus-topology data center network based on optical packet/agile circuit switching with intelligent flow management," *J. Lightw. Technol.*, vol. 33, no. 5, pp. 1063–1071, Mar. 2015.

[4] Q. Cheng, S. Rumley, M. Bahadori, and K. Bergman, "Photonic switching in high performance datacenters," *Opt. Exp.*, vol. 26, no. 12, pp. 16022–16043, 2018.

[5] K. Suzuki et al., "Low-insertion-loss and power-efficient 32 × 32 silicon photonics switch with extremely high-Δ silica PLC connector," *J. Lightw. Technol.*, vol. 37, no. 1, pp. 116–122, Jan. 2019.

[6] Y. Ma et al., "Ultralow loss single layer submicron silicon waveguide crossing for SOI optical interconnect," *Opt. Exp.*, vol. 21, no. 24, pp. 29374–29382, 2013.

[7] T. Shimoe, K. Hajikano, and K. Murakami, "Path-independent insertion loss optical space switch," in *Proc. Opt. Fiber Commun.*, 1987, Paper WB2.

[8] R. Matsumoto et al., "Fully-loaded operation of 0.29-pJ/bit wall-plug efficiency, 81.9-Tb/s throughput 32 × 32 silicon photonics switch," in *Proc. Opt. Fiber Commun. Conf.*, 2021, Paper Tu6A.2.

[9] K. Suzuki et al., "Low-loss, low-crosstalk, and large-scale optical switch based on silicon photonics," *J. Lightw. Technol.*, vol. 38, no. 2, pp. 233–239, Jan. 2020.

[10] K. Suzuki et al., "Broadband silicon photonics 8 × 8 switch based on double-Mach-Zehnder element switches," *Opt. Exp.*, vol. 25, no. 7, pp. 7538–7546, 2017.

[11] R. Konoike, H. Matsuura, K. Suzuki, H. Kawashima, and K. Ikeda, "Polarization-insensitive low-crosstalk 8 × 8 silicon photonics switch with 9 × 13.5 cm^2 control board," in *Proc. Eur. Conf. Opt. Commun.*, 2020, Paper We2C-6.

[12] K. Suzuki et al., "Nonduplicate polarization-diversity 32 × 32 silicon photonics switch based on a SiN/Si double-layer platform," *J. Lightw. Technol.*, vol. 38, no. 2, pp. 226–232, Jan. 2020.

[13] T. Goh, A. Himeno, M. Okuno, H. Takahashi, and K. Hattori, "High-extinction ratio and low-loss silica-based 8 × 8 strictly nonblocking thermooptic matrix switch," *J. Lightw. Technol.*, vol. 17, no. 7, pp. 1192–1199, Jul. 1999.

[14] K. Suzuki et al., "Recent advances in large-scale optical switches based on silicon photonics," in *Proc. Opt. Fiber Commun. Conf. Exhib.*, 2022, pp. 1–3.

[15] K. Tanizawa, K. Suzuki, K. Ikeda, S. Namiki, and H. Kawashima, "Non-duplicate polarization-diversity 8 × 8 Si-wire PILOSS switch integrated with polarization splitter-rotators," *Opt. Exp.*, vol. 25, no. 10, pp. 10885–10892, 2017.

[16] D. Dai and J. E. Bowers, "Novel concept for ultracompact polarization splitter-rotator based on silicon nanowires," *Opt. Exp.*, vol. 19, no. 11, pp. 10940–10949, 2011.

[17] K. Suzuki et al., "Wavelength (DE)MUX-and-switch based on 5.5%-Δ-silica PLC/silicon photonics hybrid platform," *J. Lightw. Technol.*, vol. 40, no. 6, pp. 1810–1814, Mar. 2022.

[18] J. Hasegawa et al., "32-port 5.5%-Δ silica-based connecting device for low-loss coupling between SMFs and silicon waveguides," in *Proc. Opt. Fiber Commun. Conf.*, 2018, Paper Tu3A.4.

[19] CWDM8 MSA GROUP, 2018. [Online]. Available: https://www.cwdm8-msa.org/

[20] IEEE 802.3bs Task Force, 2017. [Online]. Available: http://www.ieee802.org/3/bs/public/

[21] J. P. Gambino, S. A. Adderly, and J. U. Knickerbocker, "An overview of through-silicon-via technology and manufacturing challenges," *Microelectronic Eng.*, vol. 135, pp. 73–106, 2015.

[22] N. Dupuis et al., "An 8×8 silicon photonic switch module with nanosecond-scale reconfigurability," in *Proc. Opt. Fiber Commun. Conf. Postdeadline Papers*, 2020, Paper Th4A.6.

Keijiro Suzuki received the B.E. and M.E. degrees from the Department of Electrical and Electronic Engineering, Shizuoka University, Hamamatsu, Japan, in 2004 and 2006, respectively, and the Ph.D. degree from Yokohama National University (YNU), Yokohama, Japan, in 2011. After spending two years with Sumitomo Osaka Cement Co., Ltd., he joined the Department of Electrical and Computer Engineering, YNU, in 2008. After spending one year with YNU as a Postdoctoral Fellow, he joined the National Institute of Advanced Industrial Science and Technology, Tsukuba, Japan, in 2012. His research interests include photonic integrated circuits, optical switches, and nonlinear optics. He is a Member of the Optica, IEICE, and JSAP. He was awarded the Research Fellowship for Young Scientists from JSPS.

Ryotaro Konoike received the M.Eng. and Ph.D. degrees from the Department of Electronic Science and Engineering, Kyoto University, Japan, in 2014 and 2017, respectively. At Kyoto University, he studied the integration of manipulation of photons on a photonic crystal chip containing multiple coupled nanocavities. He is currently a Researcher with the National Institute of Advanced Industrial Science and Technology, Japan. His research interests include optical switches and integrated silicon optical circuits. He was the recipient of the APL Photonics Future Luminary Award in 2020.

Hiroyuki Matsuura received the B.S. and M.S. degrees in electrical engineering from the Tokyo Institute of Technology, Tokyo, Japan, in 1978 and 1980, respectively.

In 1980, he joined Yokogawa Electric Corporation, Tokyo, Japan, where he was engaged in the research on medical imaging apparatuses, high-frequency circuits, and measuring instruments. From 1990 to 1992, he was a Visiting Scholar with Stanford University, Stanford, CA, USA. From 1992 to 2011, he was engaged in the technology development of high-speed, high-frequency circuits with compound semiconductors, and business development for optical communication modules with Yokogawa Electric Corporation. Since 2011, he has been a Senior Researcher with the National Institute of Advanced Industrial Science and Technology, Tsukuba, Japan, and involved in the development of control circuits and units for next-generation optical communication devices and systems.

In 2017, he established HikariPath Communications Co., Ltd., which provides low-latency, high-resolution, and bi-directional video transmission services using optical technologies.

Mr. Matsuura is a Member of the Institute of Electronics, Information and Communication Engineers. He was the recipient of the 1988 Society of Instrument Control Engineers Best Paper Award.

Ryosuke Matsumoto (Member, IEEE) received the B.E., M.E., and Ph.D. degrees in communication engineering from Osaka University, Osaka, Japan, in 2012, 2013, and 2016, respectively. From 2016 to 2019, he was with the Mitsubishi Electric Corporation on optical access system and digital coherent transmission. In 2019, he joined the National Institute of Advanced Industrial Science and Technology, Japan, where he is currently working on optical switch system for data center networks. Dr. Matsumoto is a Member of IEEE Photonics Society, and the Institute of Electronics, Information, and Communication Engineers of Japan. He was the recipient of the 2014 IEEE Kansai Section Student Paper Award, 37th TELECOM System Technology Encouragement Award, and 2021 Young Researcher's Award from the IEICE of Japan.

Takashi Inoue received the Ph.D. degree in communications engineering from Osaka University, Osaka, Japan, in 2002. In 2002, he joined Furukawa Electric Co. Ltd., Ichihara, Japan, where he developed optical signal processing devices based on nonlinear fiber optics and silica-based planar lightwave circuits. In 2011, he joined the National Institute of Advanced Industrial Science and Technology, Tsukuba, Japan, where he is currently working on digital coherent transmission systems, signal processing techniques, and optical networks. He is a Member of the IEEE Photonics Society and IEICE Communication Society.

Shu Namiki (Fellow, IEEE) received the M.S. and Dr.Sci. degrees in applied physics from Waseda University, Tokyo, Japan, in 1988 and 1998, respectively. From 1988 to 2005, he was with Furukawa Electric Co., Ltd., where he developed award-winning high-power pump lasers and patented multiwavelength pumped-fiber Raman amplifiers. From 1994 to 1997, he was a Visiting Scientist with the Massachusetts Institute of Technology, Cambridge, MA, USA, where he studied mode-locked fiber lasers and ultra-short pulses in fibers. In 2005, he was with the National Institute of Advanced Industrial Science and Technology, Tsukuba, Japan, where he was the Chair of Executive Committee of a ten-year national project called the Vertically Integrated Center for Technologies of Optical Routing toward Ideal Energy Savings (VICTORIES) in collaboration with ten telecom-related companies, and is currently the Director of Platform Photonics Research Center. He has authored or coauthored more than 500 conference presentations, papers, book chapters, articles, and patents. His current research interests include software defined dynamic optical path networking and their enabling devices, such as nonlinear fiber-optics and silicon photonics. He was an Associate Editor and Advisory Editor for the journal *Optics Express* and the Co-Editor-in-Chief of *IEICE Transactions on Communications*. He was on the technical committee for OFC, ECOC, CLEO, OECC, and OAA and was the Program Co-Chair of OFC 2015 and General Co-Chair of OFC 2017. He is a Fellow of the Optica. He is a Member of the Institute of Electronics, Information, and Communication Engineers and Japan Society of Applied Physics.

Hitoshi Kawashima received the Ph.D. degree in chemistry from Kyoto University, Kyoto, Japan, in 1993. From 1993 to 1995, he was a Postdoctoral Fellow with the Massachusetts Institute of Technology, Cambridge, MA, USA, where he worked on pulse-shaping technology for femtosecond optical pulses. In 1995, he joined the Electrotechnical Laboratory. In 2001, the Electrotechnical Laboratory and other 14 national research laboratories were reorganized and renamed as the National Institute of Advanced Industrial Science and Technology. Since 2008, he has been working on silicon photonics and its applications to circuit switches. His research interests include integrated optics, nonlinear optics, and diagnostic techniques with ultrashort optical pulses. He is a Member of Optica, IEICE, and Japan Society of Applied Physics.

Kazuhiro Ikeda (Member, IEEE) received the B.E. and M.E. degrees in precision science from Osaka University, Suita, Japan, in 1998 and 2000, respectively, and the Ph.D. in electrical engineering (Photonics) from the University of California, San Diego (UCSD), La Jolla, CA, USA, in 2008. His doctoral thesis was on nonlinear optical responses in silicon nitride and amorphous silicon and sidewall corrugated waveguide devices, all for silicon photonics applications. From 2000 to 2004, he was with Furukawa Electric Co., Ltd., on polarization controllers and polarization mode dispersion compensators for optical fiber communications. In 2009, he was an Assistant Professor with the Graduate School of Materials Science, Nara Institute of Science and Technology, Ikoma, Japan, where he studied opto-spintronics and plasmonic microresonators for semiconductor lasers. Since 2014, he has been with the National Institute of Advanced Industrial Science and Technology, Tsukuba, Japan. His research interests include silicon photonic integrated circuits and hybrid nanophotonics on silicon. He is a Senior Member of the Optica, a Member of the IEICE, JSAP, and IEEE Photonics Society. He was the recipient of the World Cultural Council (WCC) Special Recognition 2019 and 69th Electrical Science and Technology Encouragement Award.